CAPTOPRIL ADSORPTION TO SILVER NANOSTRUCTURES

SIMONA CAVALU, SIMONA CÎNTĂ PÎNZARU**, V. CHIŞ***

*Faculty of Medicine and Pharmaceutics, University of Oradea, 10, P-ţa 1 Decembrie, 410081, Oradea, Romania scavalu@rdslink.ro
**Faculty of Physics, "Babeş-Bolyai" University, 1, M. Kogălniceanu st., Ro 400084 Cluj-Napoca, Romania

Abstract. FTIR and FT-Raman spectroscopy was used to investigate the captopril properties after different thermal treatments and storage. Vibrational behaviour in free or adsorbed state of captopril is reported here and compared to the corresponding vibrational studies upon coordination to the metal ions. The accurate vibrational assignment of the experimental observed bands was made upon DFT calculations revealing the optimized molecular geometry of this molecule.

Key words: captopril, FTIR, Raman, SERS.

INTRODUCTION

Captopril, 1-[2(S)-3-mercapto-2-methyl-1-oxopropyl]-L-proline, is the first angiotensin-converting enzyme inhibitor drug for treatment of hypertension and heart failure (Fig. 1).

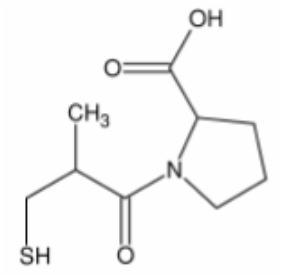

Fig. 1. Structure of captopril.

It inhibits the active sites of a zinc glycoprotein, the angiotensin converting enzyme (ACE), blocking the conversion of angiotensin I to angiotensin II, whose levels are elevated in patients with hypertension. Captopril is oxidized

Received May 2007;
in final form July 2007 .

spontaneously at its sulfhydryl group after dissolution in water to form its disulfide on the time order of hours, and is found in human urine after captopril administration [1, 5]. Like other proline-containing peptides, it normally has an equilibrium conformation between *cis* and *trans* isomers (Fig. 2), the *trans:cis* ratio for captopril at room temperature is 6:1 in aqueous solution, but the active form of captopril is the *trans* isomer when bound to the enzyme [2].

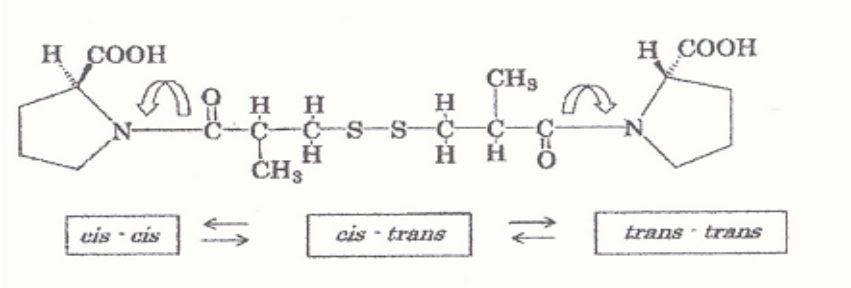

Fig. 2. Structure of captopril disulfide. The three conformations are interconvertible by rotation around the two amide bonds.

This *cis-trans* interconversion of captopril is a very important property in the pharmaceutical preparations. A number of studies have focused on the conformational analysis of captopril in solution, but there is no study on solid-state captopril [1–3, 5, 7]. Moreover, different studies dealing with its coordination properties and functional groups involved in these ligand coordinations.

For an accurate vibrational assignment of the experimental observed bands, density functional calculations (DFT) were performed in the present study for captopril molecular structure. The molecular geometry optimizations and vibrational frequencies calculations were performed with the Gaussian GO3 software package by using the B3LYP DFT method in conjunction with the split valence-shell 6-31G(d) basis set. Vibrational behaviour in free or adsorbed state of the title compound is reported here and compared to the corresponding vibrational studies upon coordination to the metal ions. FTIR and FT-Raman spectroscopy was used to investigate the captopril properties after different thermal treatments and storage.

MATERIALS AND METHODS

Captopril powder was purchased from Terapia Pharmaceuticals, Cluj-Napoca. FTIR and FT-Raman spectrum has been recorded using a Bruker EQUINOX 55 spectrometer with an integrated FRA 106S Raman module. The FTIR spectrum was registered after each thermal treatment as well as after 1h and 48h storage. After the first heating process, the sample was rapidly cooled at 25ºC

and stored for 48 h. The 1064 line of a Nd:YAG laser was applied for excitation. The detection of the Raman signal was carried out using a nitrogen cooled Ge detector and the spectral resolution was 2 cm^{-1}. SERS spectra were obtained on a Lee-Meisel Ag colloid using the final captopril concentration of 2×10^{-3} mol^{-1}.

RESULTS AND DISCUSSIONS

FTIR spectra of captopril after different treatments are shown in Fig. 3, in the range 3400–2500 and 1800–1100 cm^{-1}. In the natïve captopril powder, the peaks at 2981 and 2949 cm^{-1} were assigned to the asymmetric CH_3 and CH_2 stretching vibration, and the peak at 2877 cm^{-1} was due to the symmetric CH_3 stretching mode. The peak at 2567 cm^{-1} corresponded to the SH stretching vibration. The peaks at 1747 and 1591 cm^{-1} were assigned to the C=O stretching vibration of carboxylic acid and amide band, respectively. The peaks at 1469 and 1385 cm^{-1} were due to the asymmetric and symmetric CH_3 bending vibrations, respectively, and the peak at 1333 cm^{-1} was assigned to the OH bending vibration. The peaks at 1228–1200 cm^{-1} also corresponded to the C-O and/or CN stretching vibrations [3, 8].

Obviously, the IR spectrum for captopril at 120ºC (melt state) was significantly different from that of the native captopril (solid state) at several frequencies (see Figures 3a and 3b). After the processes of cooling and storage, these different IR peaks were gradually restored to those of the IR spectrum of native captopril, when transformed from the unstable to the stable state. The IR spectra thus turned similar for samples between Figures 3a and 3e. In general, the compound with carboxylic acid will form a dimer in the solid state, and its C=O stretching mode is always located within the range 1700–1730 cm^{-1}. The compound with the tertiary amide shows the amide C=O stretching mode in the frequency range 1680–1630 cm^{-1}. In the present study, however, the frequency of the C=O stretching of carboxylic acid in the native captopril structure at 25°C was located at the higher wavenumber of 1747 cm^{-1} and the C=O stretching of amide in solid captopril appeared at the lower frequency of 1591 cm^{-1}.

Rabenstein *et al*. [6] have found the *cis* and *trans* isomers in proline-containing peptides. They also found that the *trans* isomer of captopril in the solution was constructed by intramolecular hydrogen bonding between the carbonyl oxygen of the amide group and the carboxylic acid hydrogen. If the *trans* isomer of captopril exists in the solid state, its intermolecular hydrogen bonding should be reduced due to the formation of intramolecular hydrogen bonding in which the C=O stretching mode of carboxylic acid group and of amide group will shift to higher and lower frequencies, respectively [8]. Moreover, the C=O stretching of carboxylic acid and of amide of the *cis* isomer of captopril will fall

closer to the normal range of IR absorption. The present result is consistent with the supposition just presented and also with the X-ray crystallographic data.

After melting the solid captopril and cooling it to room temperature, we found several new frequencies at 1720 and 1643±1636 cm suggesting the coexistence of the *cis* isomer. Parallel FT-Raman and SERS measurements were made in order to investigate the possibility of determining the orientation of the captopril molecule at the colloidal nanosurface and the functional groups involved in adsorption. Captopril dissolved in distilled water (20 mg/ml) with or without UV-B irradiation was determined to form a captopril disulfide observed from the Raman band at 549 cm^{-1} in Fig. 4b, which was exacerbated by UV-B irradiation. Upon recording the Raman spectra of the powder sample, the prominent band (captopril marker) was observed at 2565 cm^{-1} and assigned to S-H stretching mode (Fig. 4a). This band is completely absent in the spectra of aqueous solutions or in all surface enhanced Raman experiments. Therefore, the S-bridging is confirmed using Raman spectroscopy.

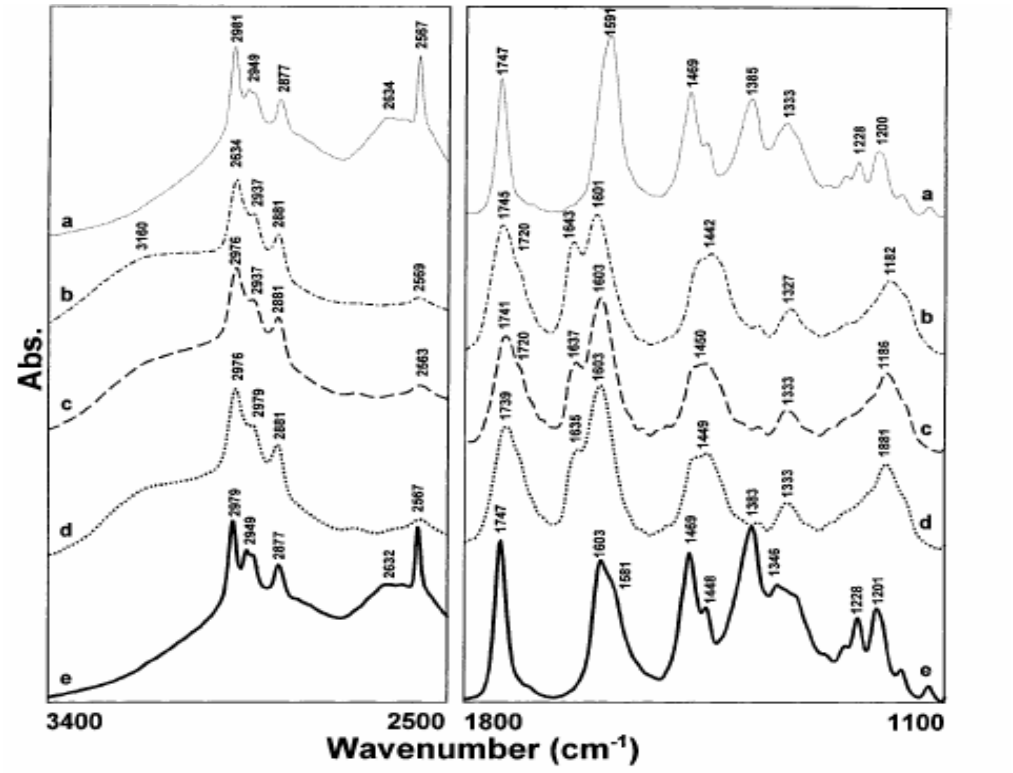

Fig. 3. Comparison of IR spectra of captopril after different thermal treatments.
a) native captopril powder, b) captopril powder after heating to 120ºC,
c) after rapid cooling to 25ºC, d) after storage for 1h, e) after storage for 48h.

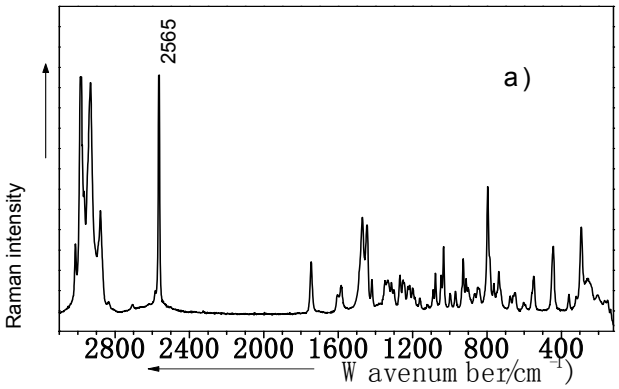

Fig. 4. a) Raman spectrum of captopril powder from Terapia Pharmaceuticals.

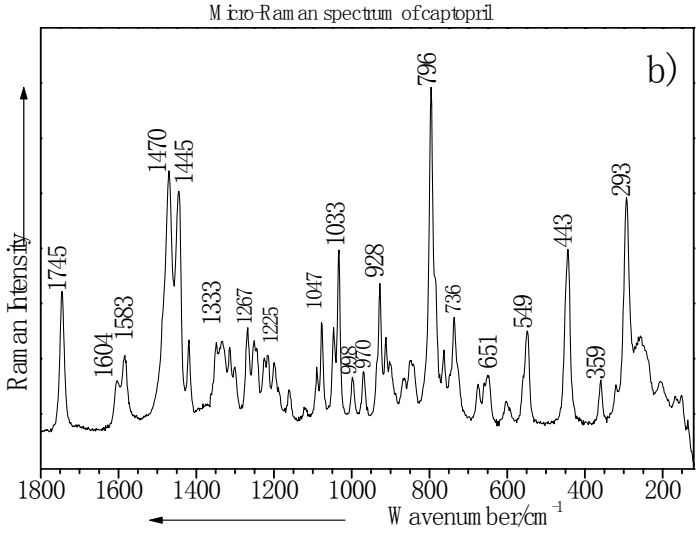

Fig. 4. b) MicroRaman spectrum of dissolved captopril 20 mg/ml in distilled water.

Surface enhanced Raman scattering was employed here in order to investigate adsorption behavior of the captopril species to a given nanostructured surface and to compare the versatility to form chemical complexes with the chemisorbed species properties. Moreover, a geometry orientation at the Ag colloidal surface would reveal the functional groups involved in adsorption. The

dominant SERS bands were observed in the 1700–200 cm^{-1} spectral range (Fig. 5). Comparing Raman and SERS spectra of captopril, large differences could be observed in band positions and relative intensities, confirming that the molecular species is chemisorbed on the Ag nanoparticles. As expected, the S-H stretching mode was absent in SERS. The dominant SERS bands were related to the deformations of the –COOH, –CH3 and –OH groups, because of adsorption. According to the surface selection rules, the orientation of these functional groups could be estimated. Furthermore, taking a closer look to the low wavenumber region of the SERS spectra, one can observe a complex spectral shape of the band 217 cm^{-1} (attributable to Ag-O stretching). Therefore, either carboxylate or –OH groups could be close enough to the Ag surface. However, from sterical point of view, the most probable geometry orientation would have the S-bridging as an axial structure lying on the surface. Therefore, the S-C stretching would adopt a more parallel orientation with respect to the surface. Consequently, the observed band at 644 cm^{-1} involving S-atoms was less enhanced.

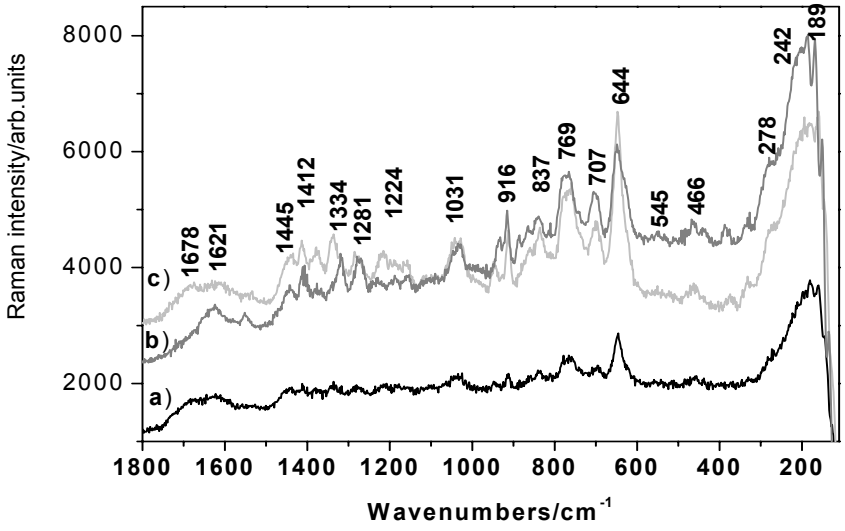

Fig. 5. SERS spectra of captopril upon increasing concentration from 2x (a) to 4 × (b) and 8 × 10^{-3} mol^{-1}.

Table 1

Selected vibrational FT-Raman and SERS data of captopril with their assignments

Calc.	I[%]	A[%]	Assignments	Exp Raman	SERS
3007	4.48	51.81	niuas(C3H2)+niuas(C4H2)	3013	
3006	11.93	18.87	niuas(CH3)	2983	
2955	6.20	51.92	nius(C3H2)+nius(C4H2)	2967	
2949	5.70	28.73	niu(C7H)	2947	
2942	4.69	48.79	nius(CH3)	2932	
2913	12.94	37.23	nius(C5H2)	2879	
2582	8.20	100.00	niu(SH)	2565	
1782	100.00	3.65	niuas(COOH)	1746	1678
1675	74.64	5.45	niu(C6O)	1604	1621
1475	1.96	7.51	D(CH3)+d(C9H2)+d(C3H2)+d(C4H2)	1470	
1463	1.64	9.07	d(C3H2)+d(C4H2)	1445	1445
1399	79.84	1.50	niu(CN)+w(CH3)+d(C7H)	1419	1412
1341	0.63	2.13	w(C5H2)+d(C2H2)	1348	
1334	7.44	0.75	d(OH)	1334	1334
1326	10.28	2.38	d(C7H)+d(C2H+d(OH)	1313	
1295	9.52	1.51	w(C9H2)+d(C7H)+w(C3H2)+d(C2H2)	1301	
1291	1.49	1.55	w(C3H2)+w(C5H2)+w(C9H2)	1268	1281
1259	1.34	5.19	t(C4H2)+d(C2H2)+w(C9H2)	1251	
1241	13.58	1.00	w(C9H2)+d(C7H)+t(C4H2)+t(C5H2)	1244	
1230	6.63	7.23	t(C5H2)+tC3H2)+d(C7H2)+d(C2H2)	1225	
1192	1.58	3.75	t(C9H2)+t(CH3)	1200	
1099	2.66	0.87	d(C8H3)+dC7H)+d(SH)+ t(C9H2)	1090	
1074	11.95	0.31	t(C3H2)+r(C5H2)+niu(C11O12)+d(OH)	1077	
1042	2.60	1.66	d(SH)+d(C7H)+niu(C7C8)	1047	
1027	1.30	2.67	t(C9H2)+d(C7H)+d(CH3)	1033	1031
1017	4.02	4.05	niu(C2C3)+niu(C4C5)+d(C2H)	998	
934	0.26	4.34	d(SH)+r(CH2)	927	916
921	2.53	2.23	d(SH)+r(CH2)	912	
898	0.80	4.49	d(SH)+r(C9H2)	901	
872	5.46	3.64	d(SH)+r(C9H2)	864	
831	1.35	1.87	d(N1C2C3)+d(SH)+r(C9H2)	842	837
804	0.81	0.79	d(SH)+r(CH2)	796	
781	0.32	12.69	niu(CS)+d(SH)+d(C6C7C9)	785	
754	11.25	1.42	g(C2C11)+d(OH)	763	769
748	4.24	2.44	g(C6O)+r(CH3)+r(CH2)+d(SH)	736	
669	4.41	0.76	g(OH)+niu(CS)+d(N1C2C3)	675	707
650	21.72	2.31	g(OH)+d(C3C4C5)+niu(CS)	659	644
604	11.74	1.94	g(OH)+d(N1C6C7)	603	
581	8.78	0.38	d(COOH)+r(CH2)	560	
548	7.00	1.32	d(C3C4C5)+d(N1C6C7)	548	545
443	0.55	1.13	d(C8C7C9)+g(SH)	444	446
333	1.63	0.07	g(CN)	359	
286	0.42	0.75	r(CH2)+g(CN)+g(CC); Ag-S, Ag-N	292	278 242

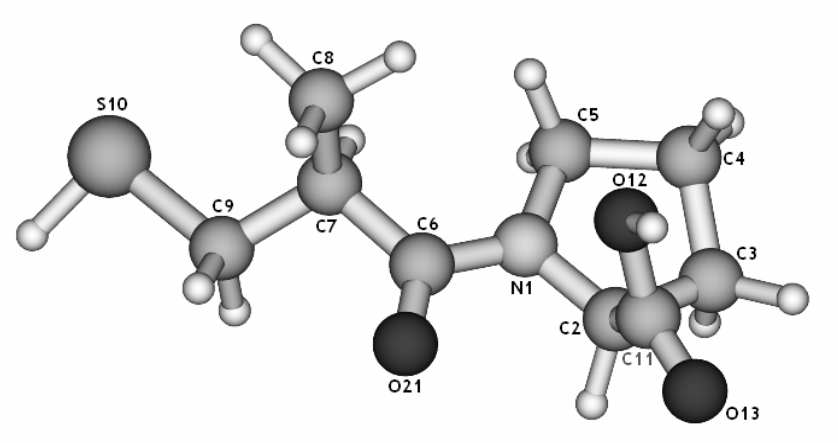

Fig. 6. The optimized geometry of captopril molecule obtained upon DFT calculations.

The exact vibrational assignment of the experimental observed bands was made upon density functional calculations (DFT) shown in Table 1. The molecular geometry optimizations (Fig. 6) and vibrational frequencies calculations were performed with the Gaussian GO3 software package by using the B3LYP DFT method in conjunction with the split valence-shell 6-31G(d) basis .

CONCLUSIONS

FTIR, Raman and SERS spectroscopy investigations on captopril in both solid and liquid state reveal the following: (a) Thiol moiety of the captopril species exhibits a marker Raman band that is completely quenched in the spectra of aqueous solution. (b) Captopril dissolved in distilled water was determined to form a captopril disulfide evidenced from the SERS spectra at 642 cm^{-1}. (c) Carboxylic acid and C=O groups were found to interact with the Ag colloidal nanoparticles more than the proline moiety, leading to a chemisorbed torsioned geometry of the disulfide bridging structure.

REFERENCES

1. CUSHMAN, D.W., M.A. ONDETTI., Design of angiotensin converting enzyme inhibitors, *Nat. Med*., 1999, **5,** 1110–1113.
2. GREE, D.S.S., I.H. HILIER, G.A. MORRIS, L. WHALLEY, Determination of the barrier to C-N bond rotation in captopril, *Magnet. Reson. Chem*., 1990, **28**, 820–823.
3. JANKOVICS, H., C. PETTINARI, F. MARCHETTI, E. KAMU, L. NAGY, S. TROYANOV, L. PELLERITO, Characterization of diorganotin (IV) complexes with captopril. The first crystallographically authenticated metal complex of this antihypertensive agent, *J. Inorg. Biochem.*, 2003, **97**, 370–376.

4. LI, M.J., S.Y. LIN, Vibrational spectroscopic studies on the disulfide formation and secondary conformational changes of captopril-HAS mixture after UVB irradiation, *Photochemistry and Photobiology*, 2005, **81** (6), 1404– 1410.
5. NISIKAVA, T., R. ABE, Y. SUDO, A. YAMADA, K. TAHARA, *Analytical Sciences*, 2004, **20**, 1395–1398.
6. RABENSTEIN, D.L., A.A. ISAB, The conformation and acid-base equilibrium of captopril in aqueous solution, *Anal. Chem.,* 1982, **54**, 526–529.
7. SANTANA MARIAPPAN, S.V., D.L. RABENSTEIN, Kinetics and thermodynamics of *cis-trans* isomerization of captopril and related compounds, *J. Org. Chem.*, 1992, **57**, 6675–6678.
8. SMITH, B., Infrared Spectral Interpretation: A Systematic Approach, Boca Raton, Florida, CRC Press, 1999.